SEM Studies of the Morphology and Chemistry of Polar Ice

PIERS R.F. BARNES,[1] ERIC W. WOLFF,[1]* DAVID C. MALLARD,[2] AND HEIDY M. MADER[2]
[1]*British Antarctic Survey, Cambridge CB3 0ET, United Kingdom*
[2]*Department of Earth Sciences, University of Bristol, Bristol BS8 1RJ, United Kingdom*

KEY WORDS Antarctic; Greenland; grain boundaries; triple junctions; soluble chemistry

ABSTRACT Determining the microphysical location of impurities in natural ice from the polar regions is necessary for understanding the physical properties of ice and for assuring the integrity of ice core records. SEM, using a cold stage and X-ray microanalytical techniques, has proved to be the most powerful method so far for undertaking such work. Methods are adapted from those used to study frozen hydrated biological material. Sublimation within the cryo-chamber is often needed in order to concentrate impurities onto a plane, but this can lead to artifacts that must be recognized. Over 100 samples from different depths and sites in Greenland and Antarctica have been examined. Typical physical features, including air bubbles, clathrate hydrates of air, and dust particles are identified. The dust is found preferentially at grain boundaries in some samples; by pinning the boundaries, it can slow grain growth. Of the soluble material, chloride seems to be found most frequently in the ice lattice. Other impurities are found at grain boundaries, and only when the bulk concentration exceeds a threshold, at triple junctions. These findings give new insights into processes determining the physical properties of ice samples and of ice sheets, and new impetus for theoretical studies of the energetics that lead to this distribution. *Microsc. Res. Tech. 62:62–69, 2003.*

INTRODUCTION

The vast majority (99%) of the natural freshwater ice on Earth is found in the polar ice sheets of Antarctica and Greenland. While the ice in these remote areas is of high purity, it is still the case that many of the physical properties of the ice caps, and of samples taken from them, are determined by the small amounts of impurity (i.e., whatever is not H_2O) that they contain. Additionally, ice cores drilled from the ice sheets have proved to be the richest source of information available for deciphering the history of our climate and atmosphere over the last several hundreds of thousands of years. Again, the changing concentrations of trace impurities in the ice provide many of the data for these climatic reconstructions.

While most studies of polar ice chemistry have measured the concentrations of impurities in the ice, it has become clear that, for understanding the physical properties of the ice (e.g., Wolff, 2000), and for assuring that the chemical records are undisturbed (Rempel et al., 2001), it is also necessary to understand the microphysical location of impurities in the ice. Are impurity ions and molecules found throughout the ice (either substituted in the lattice, or at dislocations), or are they found preferentially at grain boundaries (where two grains meet), or at triple junctions (where three grains meet)? The answer to this question is the key to understanding whether and how impurities can react together, move through the ice, or diffuse within it, all processes that would disturb the palaeoclimate record of the ice. It would also shed light on the mechanism by which electrical conduction occurs in polar ice, and almost certainly has an influence on the mechanical strength of the ice (which in turn determines the flow of entire ice sheets). It is, therefore, urgent to locate impurities within polar ice.

A number of methods can be imagined for doing such microphysical analysis (laser ablation microanalysis, Raman spectroscopy, NMR spectroscopy, use of microelectrodes to probe the grain boundaries) but only one (SEM with X-ray microanalysis) has been used systematically to probe the location of the major impurities in polar ice. The first reported analyses borrowed techniques used for studying frozen hydrated biological material to analyse a very small number of Antarctic (Mulvaney et al., 1988) and Greenland (Wolff and Mulvaney, 1990) samples. Sulfur (S) was found in high (order molar) concentrations at triple junctions in ice containing high bulk concentrations of sulfuric acid, and it was inferred that the majority of sulfuric acid in such ice resided in a network of veins containing liquid sulfuric acid/water. Such a network is an attractive way of explaining the electrical properties of polar ice (Wolff and Paren, 1984). However, in the small volume of ice observed in these early measurements it was impossible to generalize the findings to ice with lower concentrations of sulfuric acid, or to ice containing other impurities. Impurity was not seen at every triple junction, and it was not clear if this result was real or was an artefact of the ice preparation methods. Finally, the methods used were not adequate for determining whether impurity was present at grain boundaries or in the grains themselves.

It has only been in the last few years that systematic work, mainly by two teams (Barnes, 2002; Barnes et

*Correspondence to: Dr. E.W. Wolff, British Antarctic Survey, High Cross, Madingley Road, Cambridge CB3 0ET, UK. E-mail: ewwo@bas.ac.uk
Received 13 January 2003; accepted in revised form 17 April 2003
DOI 10.1002/jemt.10385
Published online in Wiley InterScience (www.interscience.wiley.com).

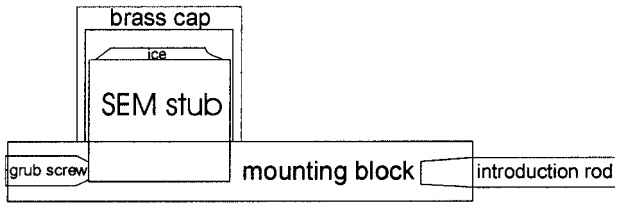

Fig. 1. Schematic of the arrangement of specimens before they are loaded into the cryo-chamber, showing the ice mounted onto the stub and covered by the brass cap.

al., 2002a,b; 2003 Cullen and Baker, 2000, 2001), has been undertaken to resolve these issues. This article describes the methods, recent observations and interpretations by one of these teams.

MATERIALS AND METHODS

SEM Techniques

Methods are described in detail elsewhere (Barnes et al., 2002b) and are only summarized here, with the addition of some comments about techniques specific to this work. The basic instrument used in this work was a Leica S360 SEM, with the addition of a four quadrant solid state back-scattered electron detector and an Oxford Instruments CT1500 cold stage. Two X-ray analysis systems were used: an Oxford Instruments INCA system with an ATW Germanium energy dispersive detector and an Oxford Instruments Microspec 400 wavelength dispersive detector with Winspec software. An Oxford Instruments cryo-transfer device was used to introduce samples to the SEM cryo-chamber. Specimens of approximately 5 mm in diameter, and up to 5 mm thick, were cut from the core using a cleaned hacksaw and scalpel. Cylindrical brass stubs of diameter 10 mm and height 8 mm were used to mount the ice, using Leit-C conducting carbon cement.

As a result of tests to determine the best way to obtain satisfactory flat surfaces, samples were cut with a sledge microtome, using a hardened steel knife, in a cold room at −20°C. Samples were then generally left to stand for a few hours in a sealed container in the cold room; this process (which we refer to as pre-etching) smooths the surface, and makes it much easier to see the location of grain boundaries and triple junctions, since grooves appear at these sites due to preferential sublimation. Pre-etching must be used with care since it obviously opens up the possibility that impurity can diffuse across the surface.

Specimens were covered with a brass cap (Fig. 1), and immersed in liquid nitrogen. The cooling outside the instrument prevents the rapid and uncontrolled surface sublimation that is inevitable if warm samples are placed into the high-vacuum environment of the SEM. The brass cap was found to be the best and simplest solution to the problem of condensation forming on the ice surface during introduction to the instrument; it completely eliminated the need to sublimate frost from the ice. Once the sample was safely installed in the airlock of the SEM cryo-chamber, the brass cap was simply tipped off for later retrieval. Samples were generally not cut in the cryo-chamber, because this low-temperature cutting produced rough fractured surfaces that were hard to interpret, and they were generally left uncoated to allow later etching, and to avoid any interferences in the X-ray analysis.

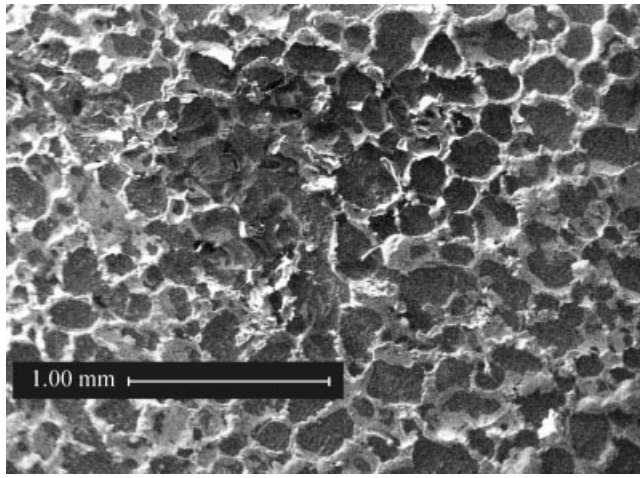

Fig. 2. NaCl skeleton after sublimation of the grain interiors. This sample was cut from the centre of ice cubes of a 1M NaCl solution frozen at −20°C, and prepared for the SEM using the same methods as the polar samples. It had been pre-etched for 3 hours and subsequently etched for ~15 minutes at −80°C. Scale bar = 1 mm.

In examining samples on the cold stage of the SEM, it is important to remember that a working hypothesis is that some of the impurities are present in a liquid or liquid-like form, above their eutectic temperatures, at grain boundaries or triple junctions at temperatures around −20°C (in the laboratory and during pre-etching) and in the field. What we see in the SEM is the structure, including the impurities, frozen into place as the samples are cooled below the eutectic temperature of all impurities during immersion in liquid nitrogen. Using present techniques, there remains some danger that impurity locations are altered during sample preparation, especially at the pre-etching stage.

Etching Techniques

Many samples were etched once inside the cryo-chamber by raising the stage temperature. Experiments using samples of known thickness showed that, at −80°C, a sublimation rate of 6.2 ± 0.4 μm min^{-1} was achieved. Etching was used principally to concentrate impurities from a given volume down onto a plane at levels high enough for analysis. For example, after etching a given volume (calculated as the exposed area multiplied by the sublimation rate and time), dust particles from that volume can be seen on the newly exposed surface.

However, especially for grain boundaries and triple junctions, it is important to bear in mind what etching is achieving when interpreting the results of it. In the simplest case, where very concentrated impurity is present at grain boundaries, etching leaves behind a skeleton that shows the grain boundary structure. This is shown in Figure 2, where a solution of 1 M NaCl was frozen to create ice with NaCl (probably at the eutectic concentration) at very thick, prominent boundaries. On etching, the NaCl skeleton has enough rigidity to re-

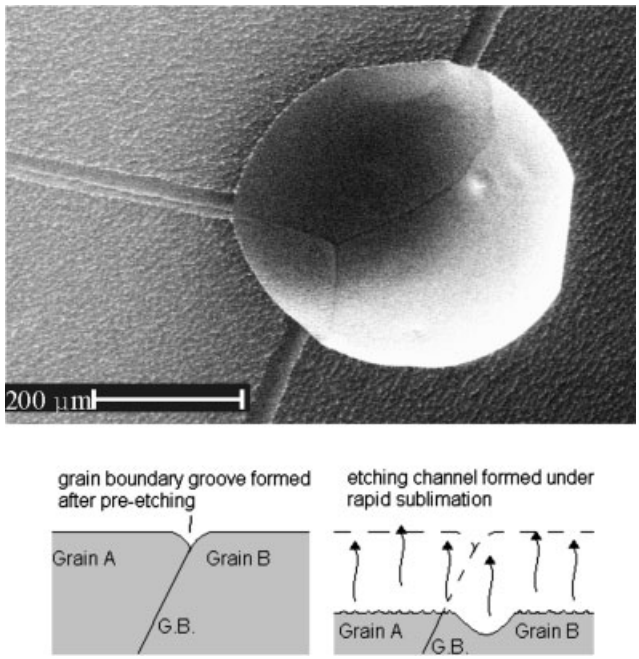

Fig. 3. Grain boundaries, air bubble and etch channels. This sample from Dome C, Antarctica, had been pre-etched and etched. Scale bar = 200 μm. Three grain boundaries (and one triple junction) are clearly seen in the air bubble. The etch channel on the left of the picture aligns with the boundary, and contains a raised filament (usually indicative of the presence of impurity). The other two etch channels are misaligned with the boundaries, and there is no sign of the grain boundary on the surface; this suggests that while the etch channel has simply moved vertically downwards, these two boundaries are not perpendicular to the surface, so that the etch channel no longer marks the boundary location (as shown bottom). Photograph courtesy of Journal of Glaciology.

main largely intact, while the purer grain interiors sublimate away, providing some insight into the three-dimensional structure of the system.

In natural samples, with much less impurity, the material will remain on the retreating surface, ending up on the final exposed plane. If a grain boundary or triple junction is close to vertical, then it is likely that the material will be able to coagulate into a line (actually seen as a filament of impurity, as discussed later) or a spot, respectively. However, if the grain boundary or junction is oblique to the direction of sublimation, then it seems probable that the material will instead be smeared into a much more diffuse area or line, respectively, and is less likely to be at a detectable level in a given analysis area. The rate of sublimation may also be important in determining whether the impurities coagulate or not. The effect of these processes can be one reason (although there are others) why impurity is not detected at all boundaries.

A further possible confusion comes in interpreting the location of grain boundaries on etched surfaces. The boundaries themselves are often hard to see, and have sometimes been inferred to be located at the position of the linear grooves seen on the surface. While these are certainly located at the boundaries before etching, this is not necessarily the case afterwards. Figure 3 shows the trough of an air bubble embedded in the surface of ice cut from a depth of 140 m in the Dome C core. The surface was pre-etched at −20°C for one day after cutting to achieve a smooth surface and clear grain boundary grooves. Once the specimen was introduced into the SEM, the surface was etched for 10 minutes at −70°C, sublimating approximately 200 μm from the specimen surface. During etching, clear channels develop on the surface at the original position of the grain boundary grooves, with a channel width about one fifth the depth of sublimed ice. However, grain boundary grooves visible in the bubble cavity—a site where less sublimation has occurred due to curvature—appear not to match the location of the surface etching channels at the top and bottom of the image. In fact, no indication could be detected on the surface of the intersection of the grain boundary with the surface at the positions expected from the bubble. Only where the grain boundary is congruent with the base of the etching channel can the intersection of the grain boundary be observed during etching (this is seen in the left-hand grain boundary of Fig. 3). In this case, a ridge or filament is forming, probably due to the coagulation of hydrated impurity salts concentrated at the boundary. There is a close correspondence between the duration of pre-etching (and hence the depth of the grain boundary grooves developed on the surface) and the depth and clarity of etching channels developed during etching in the SEM. Previous studies assumed that grooves observed on an etched surface are caused by preferential sublimation at the grain boundary (Barnes et al., 2002b; Cullen and Baker, 2001) similar to the formation of grooves caused by sublimation under quasi-equilibrium conditions (pre-etching). Figure 3 suggests that under dynamic sublimation conditions (i.e., etching as opposed to pre-etching), this is not the case; rather etching may accentuate grooves already present on the surface at the start of etching but may not follow the grain boundary. Further examples are needed to confirm our interpretation of the observations represented by Figure 3. If generally correct, the consequence would be that, unless they coincide with etching channels, grain boundaries and triple junctions on an etched surface will only be distinguishable by the fact that crystals with different orientations sometimes show different surface textures. During etching, any impurity at a grain boundary perpendicular to the surface will coagulate as a filament, co-located with the etching channel, on the retreating surface. However, impurity at a grain boundary or vein that is not parallel with the direction of etching will be spread across the retreating surface, ending up as coagulated surface spots, which will not coincide with the etching channel. Some data in previous studies using etching should be re-evaluated in light of this.

X-Ray Microanalysis

Both EDS (energy dispersive spectrometry) and WDS (wavelength dispersive spectrometry) techniques have been used. For the EDS work described in Soluble Impurities, a beam voltage of 15 kV and a current of 0.5 nA was used, with samples maintained at a temperature between −120° and −130°C. At this temperature, a very small amount of sublimation seems to reduce surface charging to a level acceptable for low-resolution imaging and qualitative (but not quantita-

tive, see Samples) analysis even though samples are uncoated. Some attempt at quantifying minimum detectable amounts of impurity in EDS was made by using artificial standards consisting of high molarity solutions frozen into the holes of track-etched polycarbonate filter papers (Reid et al., 1992). Such a system is considered to mimic to some extent the situation that might exist at triple junctions, where a high concentration channel of impurity could be present, surrounded by a medium of low conductivity material. It is less suitable as an analogue for other arrangements of impurities.

Because the detection limits of WDS are in general an order of magnitude lower than those of EDS under appropriate collection conditions, the technique of choice for quantitative X-ray micro-analysis of elements at low concentrations is still WDS. For quantitative analysis, the following conditions must be met: no (surface) charging; flat surface; stable sample targeting; no beam damage. Ideally, good standards should also be available in order to avoid the potentially prohibitively high errors of standardless analysis techniques. There are many problems with meeting these conditions and in providing appropriate homogeneous standards for ice samples. Even carefully microtomed (1 μm final cut depth) ice samples have a degree of surface roughness that is exacerbated by any subsequent etching. Any relaxation of the conditions above introduces significant errors into the matrix correction calculations and renders any results qualitative at best.

WDS analysis is usually carried out at high beam current and accelerating voltage, which causes problems due to the instability of ice and its non-conducting nature. However, WDS data have recently been collected alongside EDS data over a range of operating conditions—temperature, beam current, accelerating voltage, and analysis area—in order to assess both appropriate operating conditions for analysis of uncoated ice samples and the feasibility of using both methods in working towards accurate analysis. Some of the findings are presented here. The samples (artificial NaCl-doped ice) were prepared as in the legend for Figure 2 but were not etched.

As expected, the large boundaries containing NaCl between the ice grains produced strong signals in both EDS and WDS. In a non-charging situation, the high-energy cutoff or Duane-Hunt limit (DHL) lies at the accelerating voltage of the electron beam (Goldstein et al., 1992). A lower cutoff observed in the EDS spectrum gives an indication of the degree of charging over the collection time of the spectrum. The data showed that samples were charging significantly over the full range of conditions investigated (15 to 5 kV accelerating voltage; 5 nA to 0.5 nA beam current; −135°C to −100°C; 1 μm^2 and 4 μm^2 analysis areas). For example, with conditions of 10 kV, 0.5 nA, −100°C, and 1 μm^2 analysis area, the DHL was at ~7.73 keV rather than the expected 10 keV. At the lowest temperatures, charging was so acute that good imaging was not possible.

Despite the problems, the WDS data in Table 1 demonstrate that characteristic X-ray peak counts are still distinguishable above background for a 1 μm^2 analysis area and reasonable count times even at low accelerating voltage and beam current. The variation in peak counts and peak/background ratio (P/BG) with decreasing accelerating voltage illustrates the problems involved. At 15 kV, the high accelerating voltage leads to greater charging than at 10 kV. Higher charging reduces the landing energy of the electron beam and can cause the beam to drift across the surface; consequently, the peak and P/BG are lower at 15 kV. However, at 5 kV the overvoltage ratio is considerably lower and so although charging is reduced, the production of X-rays is significantly lower than at 10 kV due to the lesser excitation of the sample, thus reducing count statistics precision. At high accelerating voltages and high beam currents, interaction of the sample and electron beam causes localised heating leading to mass loss, which has been observed at high magnifications. Utilisation of higher temperatures to try and alleviate sample charging, by allowing greater sublimation, risks higher mass loss during analysis.

TABLE 1. Effect of different accelerating voltages on the WDS detection of Na and Cl in an ice sample containing NaCl at high concentration at grain boundaries

Accelerating voltage/kV	Element	Peak counts	P/BG ratio
15	Na	1,411	200
	Cl	298	32
10	Na	3,332	416
	Cl	698	57
5	Na	662	82
	Cl	83	8

[1]The data are for 30 seconds on peak (P) and 30 seconds on background (BG). Na with TAP and Cl with PET crystals. All data are for 0.5 nA beam current, 1 μm^2 sampling area, and −100°C.

The initial tentative findings of this study show that WDS as well as EDS produce enough counts for quantitative analyses, but neither should be used without due recognition and minimisation of the errors involved. Whichever equipment is used, further investigation is needed to pinpoint the best compromise conditions for approaching quantitative X-ray microanalysis.

Samples

More than 100 specimens have been examined from the following sites: the Dome C core, Antarctica, drilled in 1999 (75°06′S, 123°24′E, 3,233 m elevation and −54.5°C mean annual temperature), a Dronning Maud Land core drilled in 1998 (77°S, 10°W, 2,200 m elevation and −38°C mean annual temperature), surface snow collected in 1999 from the clean area near Halley station situated on the Brunt Ice Shelf (75°35′S, 26°30′W, 32 m elevation and −19.3°C mean annual temperature), and the GRIP ice core from Greenland drilled in 1990 (72°34′N, 37°37′W, 3,232 m elevation and −32°C mean annual temperature). All specimens were stored in a cold room at −20°C before cutting and examination. The samples ranged from unconsolidated firn to solid ice. All samples were from relatively acidic ice (i.e., ice that gives acidic meltwater) of Holocene age (<10 kyr) except for the Dome C samples at 501 m, and GRIP samples at 1,980 m (both around 20 kyr from the last glacial maximum) in which much of the acid has been neutralised. The four different sites were used to provide ice of varying composition for the study rather

than for the purpose of making climatic comparisons between the sites.

RESULTS
Morphology and Physical Features of Polar Ice in the SEM

Many of the features that are commonly observed in the light microscope are, of course, seen also in SEM images, and have been shown elsewhere (Barnes et al., 2002a). As already discussed, grain boundaries are easily seen in samples that have been pre-etched, due to the presence of etch channels. Fainter features running sub-parallel to the boundaries are interpreted as subgrain boundaries (faint boundaries between grain regions with different lattice orientations). In some cases, different grains appear to have different surface textures after etching, probably because the orientation of the crystal axes is different, and that allows the position of grain boundaries to be determined even when the etch channels are not a reliable guide (as discussed previously).

Spherical air bubbles, typically hundreds of microns across, are seen embedded in shallower ice; smaller microbubbles (typically 1 μm) are also seen. In deeper ice, it is known that overburden pressure changes the air bubbles into clathrate hydrate crystals, and features are observed (Fig. 4) that can be identified as the residue of such crystals after they have decomposed (due to the low pressure), expelling the air and leaving a honeycomb of residual ice (middle image). In firn, the structure of the necks that join adjacent grains can be seen, and by looking at ice from different depths, the evolution of the structure can be observed.

Insoluble dust particles (wind-blown material from other continents) are typically micron-sized in both Greenland and Antarctic ice, and are, therefore, not well resolved in light microscopes. In the SEM, typical surfaces contain very few dust particles, and it is necessary to etch the ice so that the dust from a significant volume can be observed on the resulting surface. When this is done, dust particles are difficult to distinguish at first from highlight spots that result after etching, although backscattered electron images assist in identification. X-ray microanalysis readily confirms that dust is present (Fig. 4, top, bottom) provided the particles are large enough that the detection limit is exceeded for the conditions used and for particular elements. It is possible to perform crude surveys of the number concentration and composition of the dust. In Dome C (Antarctic) ice, dust particles turn out to be strongly concentrated in grain boundary regions, whereas this seems to not always be the case in GRIP (Greenland) ice. Examples can be found (as shown by kinks in the otherwise straight boundary) where the dust is clearly pinning the grain boundary; this is predicted by theory (Weiss et al., 2002), but direct observation will strengthen the theoretical basis for understanding crystal growth rates.

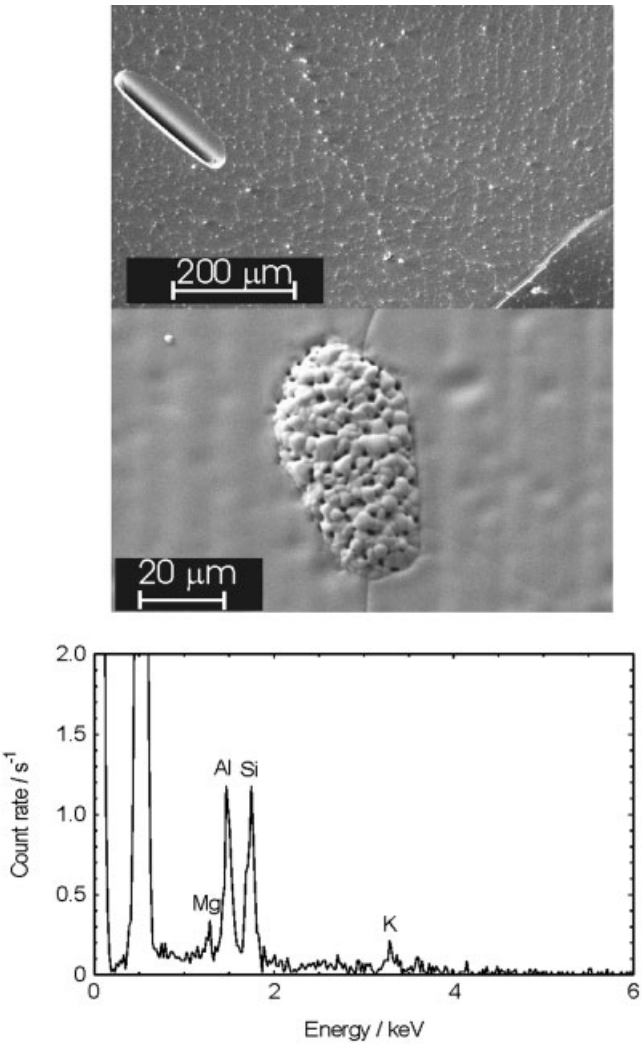

Fig. 4. Clathrates and dust particles. **Top:** GRIP (Greenland) ice sample (1,980-m depth) after etching. The hole is probably the site of a relaxation cavity formed when the ice is brought to the surface after being under great pressure; a line of dust particles (containing Ca, Si, Al, Mg) in the center of the picture has been revealed by etching. Scale bar = 200 μm. **Middle:** From close to the same depth, a pattern believed to characterize a decomposed clathrate hydrate. Scale bar = 20 μm. **Bottom:** X-ray spectrum of a typical dust particle from GRIP (Greenland), 1,980-m depth, in this case containing Mg, Al, Si, and K.

Soluble Impurities

Previous work on the location of soluble impurities in ice has looked at a small number of samples and come up with some conclusions that have been difficult to generalize. In this work, we chose samples that covered a range of sites in Greenland and Antarctica, different stages in the evolution of the ice from unconsolidated snow to aged ice, and included samples with particularly high concentrations of impurity (generally volcanic sulfate) as well as samples with typical concentrations. By analyzing over 100 specimens, our aim was to see enough examples of impurities at different locations that we could hypothesise some general rules that can be tested in future studies.

Details of the findings are presented elsewhere (Barnes and Wolff, 2003); this report summarises the findings of this work and discusses the implications.

Impurity in Bulk Ice

In some cases, after heavy etching (concentrating the impurity from a large volume onto the new surface),

impurity was observed at the bright surface etch spots, and on the edge of etch channels. The implication is that impurity originating from within the lattice has coagulated at these high spots on the surface. Chloride was by far the most common impurity found in these locations although sodium and occasionally other elements were also seen. This result is consistent with those of Cullen and Baker (Cullen and Baker, 2000; 2001) for grain interiors. (One caution about this result is that HCl may be able to sublimate along with water during etching, so that Cl could be under-represented in some cases).

For one sample, we made a crude calculation of the amount of impurity from the lattice at the etch spots. We estimated a minimum detectable amount of impurity using acids frozen into the sub-micron-sized holes in track-etched filter papers, as proposed earlier (Reid et al., 1992), and combined this with a calculation of the etched volume and number of etch spots with detectable chloride in our sample. This led to an estimate that the concentration of Cl^- in the lattice in this sample was 0.4 μM (with an uncertainty of at least 50%), the same as the total Cl^- concentration in this ice sample. It, therefore, seems that a large proportion of at least the chloride may be present in the lattice. The Cl^- ion or HCl are capable of substituting for O in the ice lattice.

In addition to the material found in etch spots, impurity (principally Na and Cl) was found in isolated inclusions, and in non-continuous linear features that are not located at grain boundaries, and that may be impurity-filled dislocations.

Bubble Surfaces

After etching, filaments of impurity (Na, Cl, and S) were found on the rim of air bubbles. We interpret this to mean that some bubble surfaces are coated with impurity. Sublimation concentrates the impurity at the retreating rim of the bubble as a ring-shaped filament.

Grain Boundaries

Filaments, similar to those observed in other studies (Cullen and Baker, 2000; 2001) were frequently seen at grain boundaries (after etching), including those at the necks between grains in unconsolidated firn. These sometimes appeared as raised ridges in etch channels (as in Fig. 3), and sometimes as "hairs" that have become partly detached from the ice surface. In the case of the necks between grains, the filament appeared buckled (e.g., Fig. 5), implying that it has retained its earlier length as the neck diameter has reduced during etching, and that it has structural rigidity. Na and Cl are the elements most commonly detected in filaments. However, there were also filaments with no detectable impurity (which may imply the presence of impurity at concentrations below the detection limit), and apparent boundary locations with no filaments, or with discontinuous filaments.

Triple Junctions

Triple junctions were frequently seen to be of small size, and containing no detectable impurity, except where they are the simple junction of three grain boundary filaments. However, in a few cases, where the bulk sulfate concentration was particularly high (in sulfate peaks arising from the fallout of volcanic acid), S was observed at triple junctions, and the junctions themselves were of the order of 1 μm across (e.g., Fig. 6). Filled triple junctions were observed only for bulk sulfate concentrations > 1.6 μM (although we would expect the critical concentration to depend on grain size). The apparent dimensions of triple junctions on some pre-etched surfaces may be exaggerated as the pre-etching presumably causes the impurity from the length of vein that has been exposed during sublimation under these conditions to be retained in the depression at the junction.

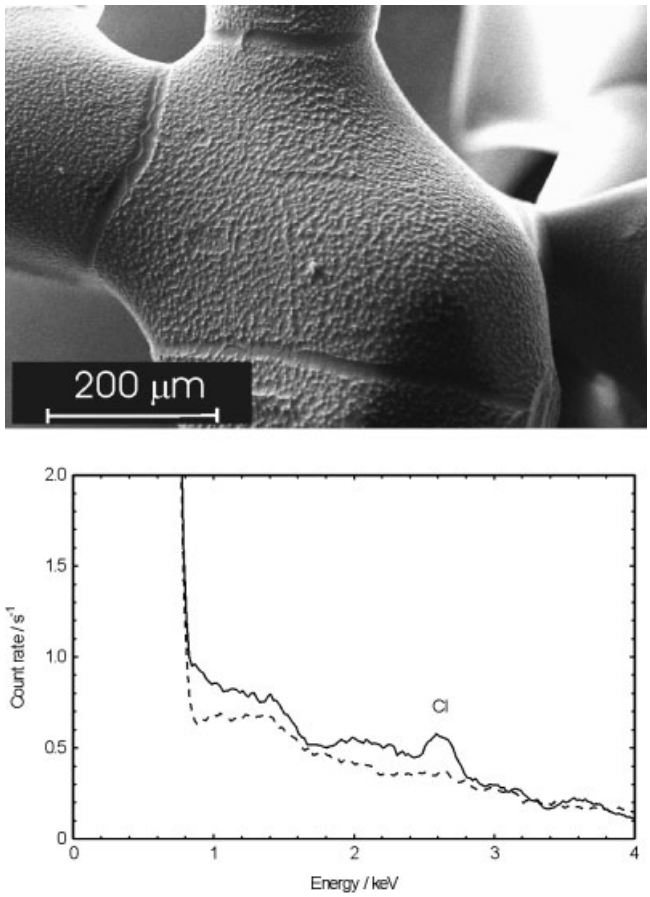

Fig. 5. **Top:** Snow from 25 cm depth at Dome C, after etching. The central grain is connected by necks to other grains (three necks are visible facing the microscope). There is a clear filament at one of the grain boundary necks, but not the others. **Bottom:** Cl was present in the X-ray spectrum for the filament (solid line) but not in that of the general background (dashed line). Scale bar = 200 μm.

DISCUSSION AND CONCLUSION

Using the findings above, and also bearing in mind the findings of earlier studies (Cullen and Baker, 2000, 2001; Mulvaney et al., 1988), we can suggest that the preferred locations are as follows:

1. Most chloride sits in the lattice where it can be incorporated substitutionally.
2. Other elements can be located at dislocations and inclusions in the ice.

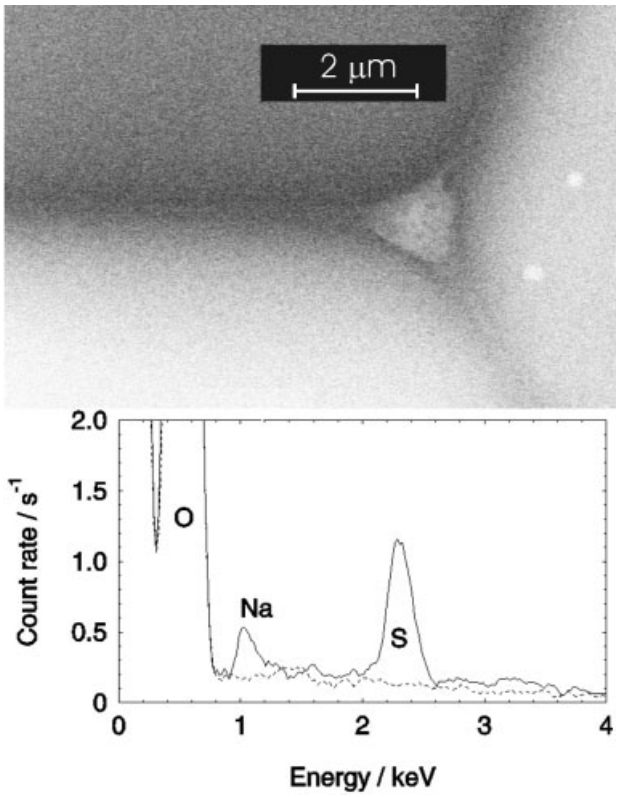

Fig. 6. **Top:** Close-up of ice from 218.95-m depth at Dome C. Scale bar = 2.0 μm. A triple junction is clearly visible. **Bottom:** The X-ray spectrum from the triple junction shows that S and trace Na is present there (solid line), whereas there is no detectable signal away from the junction (dashed line).

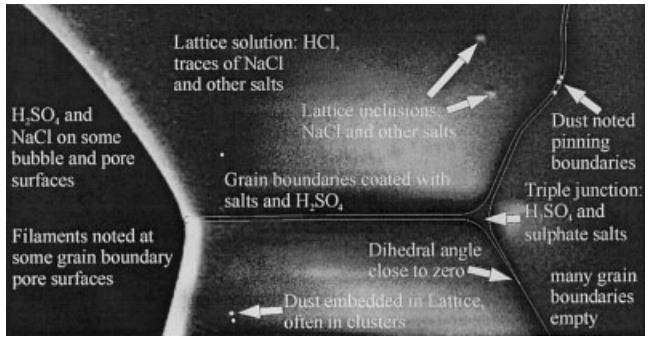

Fig. 7. A schematic depicting the general distribution and observations of impurities in cold polar ice.

3. Grain boundaries and bubble surfaces are preferred locations for many impurities. However, a simple calculation shows that, for impurity concentrations and grain boundary areas typical for central Antarctica (for example), the impurity is sufficient to coat only a few percent of the boundaries with a monolayer, even when diluted to well below the eutectic concentration. We should not, therefore, expect the grain boundary impurity to behave in a typical liquid-like fashion, nor should we expect all surfaces to be covered. Which surfaces are covered is expected to be determined by energetic considerations.
4. In samples with particularly high impurity concentration, impurity is found at triple junctions. We suggest that a monolayer of impurity (hydrated to an unknown degree but to at least the eutectic composition) at grain boundaries is energetically favourable, but that once all boundaries are saturated, triple junctions start to fill.

Figure 7 is a schematic showing the features summarized in this report. The ideas represented by this distribution of impurities are consistent with all the data obtained so far, and provide a plausible explanation for why impurity is seen at some junctions and boundaries but not all. They also suggest some tests that could be made to substantiate these conclusions. For example, further samples should be studied where high sulfate peaks are surrounded by ice of lower bulk concentration to determine whether it is correct that S is found at triple junctions only above a certain bulk impurity threshold. Similarly, studies of ice from coastal areas with high sea salt concentration should be carried out to determine what proportion of Cl is in the lattice, and whether grain boundaries will fill with Na and Cl (as has been shown to occur in highly concentrated artificial samples grown at −20°C; Fig. 2), and whether triple junctions will start to fill also for NaCl above a certain bulk concentration.

Insufficient samples have been investigated to determine clearly whether impurity locations are altered depending on whether the impurity can reside in the ice as a liquid (above the eutectic temperature). For example, we may find a different distribution for warmer sites (ice temperature above the NaCl eutectic), than for cold sites. Equally, we may find a different result for alkaline ice (such as from the Greenland ice of the last glacial maximum) than for acidic ice, as different salts dominate the chemistry. For these purposes, combined studies of artificial (doped) ice, temperate ice, and polar ice, will be needed.

Our findings challenge previous ideas that it is always thermodynamically preferred for impurity to reside at triple junctions rather than at grain boundaries (Mader, 1992; Wolff and Paren, 1984). Our data suggest instead that impurities segregate first to grain boundaries, and then only when these are saturated, to triple junctions. This implies that there is an energetic advantage to separating ice grains with different crystal orientations by a monomolecular layer of impurity. Theoretical work is needed to test this idea.

Finally, our results have strong implications for the physical properties of ice, both when sampled as an ice core, and in bulk in the ice sheet. For example, the presence of impurities at grain boundaries allows electrical conduction to occur through the boundary films, but our hypotheses imply a change to conduction through triple junction veins in very concentrated ice. Theories about diffusion, movement of impurities, and mechanical properties will also have to take account of the effects of many impurities being present at the grain boundaries.

Our understanding of the way different features manifest themselves in the SEM now seems sufficient

to carry out the studies listed above. However, quantification of the impurities by location remains a challenge. In addition, it would be of great benefit to develop further techniques to address the questions posed here, and to avoid some of the artifacts that are inevitable with present techniques.

ACKNOWLEDGMENTS

We thank Ken Robinson and Jon Ward for assistance with use of the SEM, and the teams that have collected each of the ice cores used in this article. Part of this work is a contribution to the "European Project for Ice Coring in Antarctica" (EPICA), a joint ESF (European Science Foundation)/EC scientific programme, funded by the European Commission and by national contributions from Belgium, Denmark, France, Germany, Italy, the Netherlands, Norway, Sweden, Switzerland, and the United Kingdom. This is EPICA publication no. 60.

REFERENCES

Barnes PRF. 2002. The location of impurities in polar ice. Open University, Milton Keynes: UK, Ph. D. thesis. 136 pp.

Barnes PRF, Mulvaney R, Robinson K, Wolff EW. 2002a. Observations of polar ice from the Holocene and the last glacial period using the scanning electron microscope. Ann Glaciol 35:559–566.

Barnes PRF, Mulvaney R, Wolff EW, Robinson K. 2002b. A technique for the examination of polar ice using the scanning electron microscope. J Microsc 205:118–124.

Cullen D, Baker I. 2000. The chemistry of grain boundaries in Greenland ice. J Glaciol 46:703–706.

Cullen D, Baker I. 2001. Observation of impurities in ice. Microsc Res Tech 55:198–207.

Goldstein JI, Newbury DE, Echlin P, Joy DC, Romig AD Jr, Lyman CE, Fiori C, Lifshin E. 1992. Scanning electron microscopy and X-ray microanalysis: a text for biologists, materials scientists, and geologists. New York: Plenum Press. 840 pp.

Mader HM. 1992. The thermal behaviour of the water-vein system in polycrystalline ice. J Glaciol 38:359–374.

Mulvaney R, Wolff EW, Oates K. 1988. Sulphuric acid at grain boundaries in Antarctic ice. Nature 331:247–249.

Reid AP, Potts WTW, Oates K, Mulvaney R, Wolff EW. 1992. Preparation of aqueous standards for low temperature X-ray microanalysis. Microsc Res Tech 22:207–211.

Rempel AW, Waddington ED, Wettlaufer JS, Worster MG. 2001. Possible displacement of the climate signal in ancient ice by premelting and anomalous diffusion. Nature 411:568–571.

Weiss J, Vidot J, Gay M, Arnaud L, Duval P, Petit JR. 2002. Dome Concordia ice microstructure: impurities effect on grain growth. Ann Glaciol 35:552–558.

Wolff E, Mulvaney R. 1990. Impurity distributions in ice under different environmental conditions (Abstract). Ann Glaciol 14:362.

Wolff EW, Paren JG. 1984. A two-phase model of electrical conduction in polar ice sheets. J Geophys Res 89:9433–9438.

Wolff EW. 2000. Electrical stratigraphy of polar ice cores: principles, methods, and findings. In: Hondoh T, editor. Physics of ice core records. Sapporo, Japan: Hokkaido University Press. p 155–171.